Long-Term Monitoring of Cable Tension Force in Cable-stayed Bridges using the Vibration Method. The Case Study of Binh Bridge, Vietnam

Ha Hoang
Faculty of Civil Engineering, University of Transport and Communications, Hanoi, Vietnam
hahoang@utc.edu.vn

Vu Hoang
University of Transport Technology, Hanoi, Vietnam
vuhoang@utt.edu.vn

Duong Huong Nguyen
Faculty of Bridges and Roads, Hanoi University of Civil Engineering, Hanoi, Vietnam
duongnh2@huce.edu.vn (corresponding author)

Received: 27 November 2024 | Revised: 24 December 2024 | Accepted: 1 January 2025

 DOI: https://doi.org/10.48084/etasr.9737

ABSTRACT

The tension force of a cable is an important parameter used to ensure the stable and safe working of cable-stayed bridges. This parameter needs to be strictly controlled throughout the operation of the bridge by installing direct force measurement sensors or indirect determination methods through analyzing vibration data of the oblique cables. This article introduces a method for predicting the cable tension value of a cable-stayed bridge using vibration-based data ready for application to in-service cable-stayed bridges. A method is proposed for calculating the effective length of stay cables while considering the influence of damping devices to improve the accuracy of cable tension assessment. The database to verify the model is a series of data on vibration testing in 32/80 cables of the Binh Bridge (Hai Phong) through inspections from 2007 to 2019. The bridge was damaged in 2010 and was completely repaired in 2012. The tension force monitoring during the damaged event, compared with that before and after the repair gives realizable results. The tension force was reduced over time and was recovered after the repair. Using vibration data to estimate the tension force is a fast and cost-effective method that helps minimizing risks during the exploitation and operation of cable-stayed bridges.

Keywords-tension force; vibration-based method; cable-stayed bridge; long-term monitoring

I. INTRODUCTION

A cable is one the most important structural components of the cable-stayed bridge structure due to its load resistance and vibrate behavior. The tension forces in the cable are created during construction to ensure the cable is properly tensioned and the structure remains stable throughout its lifetime. When in use, the cable force can change due to relaxing, deformed structure, and moving anchor. Therefore, the force in the cable-stayed bridge should be examined and controlled. There are two methods to control the tension force in the cable:

- Direct method using a load cell. The load cell is attached directly to the bridge cable. The cable stress and anchor deflection can be used to determine the tension load in the cable [1].
- Indirect method: measuring cable characteristics such as stress [2], strain [3], and the cable natural frequencies [4-6]. Accelerometers are attached to measure the cable vibration. The vibration data can be analyzed to determine the tension force and other structural characteristics [7].

The direct method can give more accurate results, albeit with higher cost. The cable usually has a significant length and there is a limited number of cables that this method can be applied to. For cables with normal lengths and cables in the small-span cable-stayed bridge, often indirect methods are applied. The vibration-based method that estimates cable force using its natural frequencies has been extensively employed. Practical formulas using vibration measurement data have been proposed and have proved their accuracy by comparing the

measured and the calculated values from the finite element method [8]. In this research, the tension force is calculated based on cable's natural frequency. Those formulations have been widely applied in Japan. Some research has proposed practical formula estimation if the axial rigidity and flexural rigidity are known a priori [9-11]. Artificial Neural Networks (ANNs) combined with vibration-based methods have been proposed for the estimation of the cable force avoiding mathematical calculations [12]. In [13], an optimization ANN model is established. In this model, natural frequencies, cable length, flexural stiffness, and density are considered as input data and the output data is the cable force. High accuracy is obtained whereas and the method has a wide range of applications [13]. Monitoring systems using deep learning and wireless smart sensors are proposed in [14, 15] to calculate the tension forces.

Determining the natural frequencies from the vibration method is affected by environmental conditions such as temperature, wind load, equipment, and humans. Various weather conditions should be considered for the estimation of the cable tension forces [16]. Moreover, the cable configuration is complex, and the cable's natural frequency is affected by bending stiffness, cable deformation, and angle [8, 12]. Therefore, to correctly calculate the tension force in a cable, the vibration measurement data need to be continuously monitored under construction and traffic use. Many cable-stayed bridges are equipped with dampers to manage the impact of vibration. These devices alter the seismic resistance attributes and the effective length of the stay cables. As a result, the technical parameters of the cables must be taken into account in the analysis of cable tension. Cable force is considered as a health indicator for both the cable and the superstructure of the cable-stayed bridge. As a developing country, Vietnam has a rapidly developing infrastructure system, while many cable-stayed bridges need health monitoring. Binh bridge is one such bridge. The bridge has been in service since 2005. In 2010, in the Conson storm, two big ships collided with the bridge and the cables were ruptured. The objective of this research is to estimate the cable force during its lifetime, before and after the corrupted event. The cable forces have been estimated using practical formulas that have been specifically adjusted for the Binh bridge and other existing bridges.

(a) (b)

Fig. 1. Direct and indirect methods used to determine the tension force in Vietnam. (a) Load cell, (b) vibration measurement.

II. CABLE TENSION ESTIMATION USING THE VIBRATION METHOD

Consider the cable shown in Figure 2. The global coordinate system is defined as the x-axis along the cable chord and the y-axis at the perpendicular direction. Assume that only bending stiffness is considered and the tension force T is constant over the entire cable. The equation of motion of this cable can be expressed as [17]:

$$EI\frac{\partial^4 v(x,t)}{\partial x^4} - T\frac{\partial^2 v(x,t)}{\partial x^2} - h(t)\frac{\partial^2 y}{\partial x^2} + \frac{w}{g}\frac{\partial^2 v(x,t)}{\partial t^2} = 0 \quad (1)$$

where EI is the flexural rigidity, $v(x,t)$ is the cable in plane motion, $h(t)$ is the vibration tension force in the cable, w is the weight per unit of the cable, and g is the gravity.

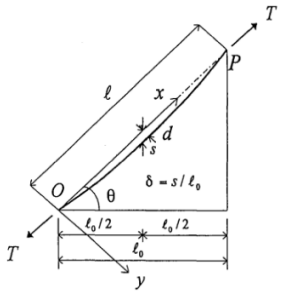

Fig. 2. The model of the inclined cable.

Assuming that $v(x,t) \ll y$ and the cable deformation is the parabolic line, (1) can be rewritten as:

$$EI\frac{\partial^4 v(x,t)}{\partial x^4} - T\frac{\partial^2 v(x,t)}{\partial x^2} + \frac{w}{g}\frac{\partial^2 v(x,t)}{\partial t^2} = \frac{8d}{\ell^2}h(t) \quad (2)$$

For high order mode, $h(t)$ present small effect even if T is a small force. Therefore, (2) is approximated as:

$$EI\frac{\partial^4 v(x,t)}{\partial x^4} - T\frac{\partial^2 v(x,t)}{\partial x^2} + \frac{w}{g}\frac{\partial^2 v(x,t)}{\partial t^2} = 0 \quad (3)$$

Authors in [8] solved (3) with some approximate parameters. The results of tension force are presented below:

- Case 1: Use mode 1 for small cable deformation $(3 \le \Gamma)$:

$$T = \frac{4w\,(f_1\,\ell)^2}{g}\left[1 - 2.20\frac{C}{f_1} - 0{,}550\,\left(\frac{C}{f_1}\right)^2\right]$$

$$\text{when}\,(17 \le \xi) \quad (4)$$

$$T = \frac{4w\,(f_1\,\ell)^2}{g}\left[0.865 - 11.60\,\left(\frac{C}{f_1}\right)^2\right]$$

$$\text{when}\,(6 \le \xi \le 17) \quad (5)$$

$$T = \frac{4w\,(f_1\,\ell)^2}{g}\left[0.828 - 10.50\,\left(\frac{C}{f_1}\right)^2\right]$$

$$\text{when}\,(0 \le \xi \le 6) \quad (6)$$

- Case 2: Use mode 2 for small cable deformation ($\Gamma \le 3$):

$$T = \frac{w\,(f_2\,\ell)^2}{g}\left[1 - 4.40\frac{C}{f_2} - 1.10\,\left(\frac{C}{f_2}\right)^2\right]$$

when $(60 \le \xi)$ (7)

$$T = \frac{w\,(f_2\,\ell)^2}{g}\left[1.03 - 6.33\frac{C}{f_2} - 1.58\,\left(\frac{C}{f_2}\right)^2\right]$$

when $(17 \le \xi \le 60)$ (8)

$$T = \frac{w\,(f_2\,\ell)^2}{g}\left[0.882 - 85.0\,\left(\frac{C}{f_2}\right)^2\right]$$

when $(0 \le \xi \le 17)$ (9)

- Case 3: Use high mode order (mode order >2):

$$T = \frac{4w\,(f_n.\ell)^2}{n^2 g}\left[1 - 2.20\,\frac{n\,C}{f_n}\right]$$

when $(200 \le \xi)$ (10)

Equations (2)-(10) are well known and presented in [8] to establish the cable force of cables in arch bridges. This research recommends the use of short equations for fast calculation and easy application for in-service bridges and using only the first mode:

- Case 1: Neglect the cable deformation:

$$T = \frac{4\,w\,(f_1\,\ell)^2}{g} \quad (11)$$

- Case 2: Consider the cable deformation:

$$T = \frac{4\,w\,(f_1\,\ell)^2}{g}\left[0{,}857 - 10.89\,\left(\frac{C}{f_1}\right)^2\right]$$

when $(3 \le \xi \langle 17)$ (12)

$$T = \frac{4\,w\,(f_1\,\ell)^2}{g}\left[1 - 2.20\,\left(\frac{C}{f_1}\right) - 2.00\,\left(\frac{C}{f_1}\right)^2\right]$$

when $17 \le \xi$ (13)

where ξ, C, and Γ are no unit parameters and are calculated as follows:

$$\xi = \sqrt{\frac{T}{EI}}\,\ell \quad (14)$$

$$C = \sqrt{\frac{EIg}{w\,\ell^4}} \quad (15)$$

$$\Gamma = \sqrt{\frac{w\ell}{(128\,EA\delta^3\cos^5\theta}}\quad\frac{0.31\xi + 0.5}{0.31\xi - 0.5} \quad (16)$$

where T is the tension force in the cable (kN), f_i is the natural frequency of the cable corresponding to mode order i, ℓ is the cable length, A is the cable area, δ is the ratio between cable deflection and cable length $\delta = s/\ell$, and θ is the angle of the cable.

III. THE CASE STUDY OF BINH BRIDGE

A. Binh Bridge

Binh bridge is located in Hai Phong province, Vietnam (Figure 3). The bridge was constructed in 2005 with financial support from the Japanese government. The bridge has three main spans (160 m mid-span and 100 m for each side-span). The slab width is 22.5 m and the girder is made of steel. The girder's height at bearing is 2.75 m and the middle span is 1.75 m. The concrete slab is 26 cm high. Two concrete pylons have 77.622 m height from the bottom of the structure and 101.6 m from the foundation.

Fig. 3. The Binh Bridge.

The supper structure is supported by two cable systems. Each cable system has 40 cables with symmetric distribution along two pylons. The cable is made of 7 mm diameter wire PWS (Parallel Wire System). The ultimate strength is 1570 N/mm^2 and the elastic modulus E is 196000 N/mm^2. The structural health monitoring period for the bridge is 5 years. Because of the implicated cost, 16 cable pairs were chosen to measure the vibration. Those cables included: four longest cables (C1a/C1b, C20a/C20b, C21a/C21b, C40a/C40b), four shortest cables (C10a/C10b, C11a/C11b, C30a/C30b, C31a/C31b), and others (C4a/C4b,C7a/C7b, C14a/C14b, C17a/C17b, C24a/C24b, C27a/C27b, C34a/C34b, C37a/C37b). In this nomenclature, Cxa is the cable upstream and Cxb is the cable downstream.

On the night of July 17, 2010, Typhoon Conson made landfall in Hai Phong. Three large transport ships, including the Shinsung Accord (Korea, 17500 tons, launched in June 2010), along with two container ships under repair—Vinashin Express 01 and Vinashin Orient—were anchored at Bach Dang Shipyard, approximately 500 m from the Binh Bridge. The strong winds and currents caused these ships to drift upstream, colliding with the structure of the Binh Bridge at positions between spans C23 and C29 on the downstream side.

The collision involving Vinashin Express 01 resulted in damage to the bridge. Specifically, part of the concrete deck was broken, and the railing was damaged. Additionally, the HDPE sheath of cable C23a was torn over a 3 m section, while cable C24a sustained an 8 m tear, as illustrated in Figure 4. Two other ships became stranded beneath the bridge between cables C28a and C29a, which caused 22.5 m of twisting damage to some sections of the downstream steel girder, leading to deformation and tearing of the main girder's side. Following the incident, the bridge operated under a restricted load capacity until repairs were completed in November 2012. After the repairs, the operating mode was restored to the normal design load. Cables C23a and C24a were replaced during the repair process. Once the repairs were finished, measurements were conducted to assess the technical parameters and natural frequency of the bridge. This evaluation included estimating and comparing the cable forces before and after the repairs to determine the bridge's structural integrity.

Fig. 4. General arrangement of Binh Bridge and the location of the bridge damage in 2010. (a) a. In 2010, when damaged, (b) in 2012, after repairs.

In 2010 and 2011, evaluated the tension condition of the cables was evaluated in their unrepaired state. The cables located near the collision site were designated for additional tension assessments. These included the following pairs: C22a/C22b, C23a/C23b, C25a/C25b, C28a/C28b, and C29a/C29b. In early 2012, a small-scale repair of the bridge was conducted. This involved cutting and welding to replace the lower flange and vertical rib sections of the warped steel girder, as well as replacing cables 23a and 24a due to damaged HDPE sheaths. After these repairs were completed, the tension in the stay cables was re-evaluated in 2012, 2019, and 2023.

B. Analyzing the Tension Cable Force with the Vibration Method

The formulas for evaluating the tension force proposed by Zui et. al since 1996 have been experimentally verified by experimental models with an error of less than 4% [8]. However, when applied to evaluate the cable tension force for real bridges, many authors have agreed that the applied formulas achieve satisfactory accuracy [18, 19]. The identified causes of error are: i) the experimental formulas assume that both ends of the cable are rigid whereas the boundary conditions at the two ends of the actual cable can be joints or elastic clamps, ii) the formula uses a piecewise function based on the value of ξ, however, this value requires an unknown cable tension force T for calculation, so it is often necessary to base on the measured frequency to calculate T according to (11) and perform iterative calculations, iii) the above formula often uses fundamental frequencies for calculation. The parameters for calculating the oscillation of the cable-stayed bridge do not actually take into account the influence of the damping device.

The vibration method is used to analyze the tension load in some cables in Binh bridge using (7). Table I shows the tension load on these cables calculated by the vibration method (T_2^*) and measured by load cells attached on cable anchors (T_0). Large differences between 20.47% and 25.07 % are recognized. In this work, the completion records of Binh bridge were used to evaluate the actual cable tension parameters after construction (T_0) and consider the influence of the dampers on the cable vibration.

TABLE I. TENSION FORCE OF THE CABLES

Cable label	**Γ**	T_0	f_2 **(2005)**	T_2^*	$\frac{T_2^*}{T_0}$
	-	kN	Hz	kN	(%)
C20a	0.003	3352	1.794	4145	23.66
C20b			1.804	4191	25.04
C21a	0.003	3342	1.794	4145	24.03
C21b			1.768	4026	20.47

There may be many reasons for the error in the cable tension analyzed by the vibration method and measured by load cells, and attention should be paid to the actual free oscillation length of the cable. The damper devices at the two ends of the cable have quite long metal guide tubes, high stiffness, and rubber stoppers to reduce the free oscillation length of the cable. Authors in [18] proposed (17) to calculate the effective length of the cable using a damper:

$$L_1 = \ell - d \tag{17}$$

where L_1 is the effective length, ℓ is the length of the cable, and d is the diameter of the cable.

The free length of the cable is measured as the distance between the damper rubber pad in the girder and the damper rubber pad in the bridge tower, as the metal guide tube provides significant stiffness. The effective length of the cable is calculated by:

$$L_1 = \ell - SLG - SLT \quad (18)$$

L_1 is then used to calculate the tension force with (7). Finite element method was used to calculate the tension force f_i^F, and discuss the differences between the measurement T_0^i and the calculated results using the vibration method. Table III presents a comparison between f_1, f_2, the FE frequencies f_1^F and f_2^F, and the corresponding deviations ranging from -0.11% to 5.56%. This result can be considered satisfactory when considering other causes such as increased tension due to wind, temperature, or errors due to the human factor and the measuring equipment. Replacing f_1^F, f_2^F in (7) and (13) acquired the results T_1^F, T_2^F that were compared with the measured tension force T_0^i with differences ranging from -1.23% to 2.06%. Therefore, the FE method is considered reliable. The high accuracy when replacing f_1^F in (13) shows that the proposed method has been adapted to be more realistic than the original formulas of [8].

Table II presents the tension force using (7) and (13) T_1 based on f_1, T_2 based on f_2, Finite Element (FE) method (T_F), and a comparison with the measurement results (T_0). The results proved that when considering the influence of the damper device and effective length L_1, the results are more consistent with the actual tension in the cable with an error ranging from 5.81 to 11.07%. The inverse calculation is also performed by basing on the measurement frequency f_2 using the FE method to deduce the cable tension T_F, which is a value that is considered to be highly reliable. The comparison also shows that the cable tension value calculated by (7) and (13) deviates from the T_F tension by about 0.08% to -1.36%, demonstrating the reliability of the experimental formulas. The tension deviation due to using L_1 is calculated by:

$$\Delta T_L = \frac{T_2 - T_{2-1}}{T_2} = 1 - \frac{L_1^2\left[1 - 4.4\frac{C}{f_2} - 1.1\left(\frac{C}{f_2}\right)^2\right]}{\ell^2\left[1 - 4.4\frac{C^*}{f_2} - 1.1\left(\frac{C^*}{f_2}\right)^2\right]} \times 100\% \quad (19)$$

The analysis of the cable tension error components presented in Table IV shows that the main reason is that the determination of the oscillation length parameter of the wire is not in accordance to the reality. Another reason is that it is impossible to fully consider the factors affecting the measurement conditions such as wind and temperature. In Table V, the difference between the actual tension T_0 and the estimated tension by the oscillation method from the measurement results $\overline{T}_1^{07}$ or $\overline{T}_2^{07}$ in 2005 can be seen.

TABLE II. TENSION FORCE OF THE CABLE USING THE VIBRATION METHOD WITH EFFECTIVE LENGTH IN 2005

Cable	ℓ	SLG (SLT)	L_1	C	ξ	Γ	T_0	Based on f_2						Based on f_1			
								f_2	FEM		(7)			FEM	(13)		
									T_F	$\frac{T_F}{T_0}$	T_2	$\frac{T_2}{T_0}$	$\frac{T_2}{T_F}$	f_1	T_1	$\frac{T_1}{T_0}$	$\frac{T_1}{T_F}$
	(m)	(m)	(m)	-	-	-	(kN)	(Hz)	(kN)	(%)	(kN)	(%)	(%)	(Hz)	(kN)	(%)	(%)
C20a	137.420	6.405 (1.98)	129.035	9.30 × 10^{-3}	182	0.003	3352	1.794	3682	9.84	3641	8.6	-1.11	0.897	3641	8.62	-1.11
C20b								1.804	3726	11.16	3682	9.84	1.18	0.907	3723	11.07	0.08
C21a							3342	1.794	3682	10.17	3641	8.62	-0.73	0.899	3657	8.61	-0.68
C21b								1.768	3585	7.27	3536	5.81	-1.36	0.886	3552	6.29	-0.92

TABLE III. TENSION FORCE OF THE CABLE USING EFFECTIVE LENGTH AND FREQUENCY FROM FINITE ELEMENT METHOD

Cable	T_0	Frequency		Measured frequency (2005)				Based on f_2^F FEM		Based on f_2^F (7)		Based on f_1^F (13)		
		f_2^F	f_1^F	f_2	f_2/f_2^F	f_1	f_1/f_1^F	T_F^F	$\frac{T_F^F}{T_0}$	T_2^F	$\frac{T_2^F}{T_0}$	T_1^F	$\frac{T_1^F}{T_0}$	$\frac{T_1^F}{T_2^F}$
	(kN)	(Hz)	(Hz)	(Hz)	(%)	(Hz)	(%)	(kN)	(%)	(kN)	(%)	(kN)	(%)	(%)
C20a	3352	1.709	0.868	1.794	4.97	0.897	3.34	3350	-0.06	3312	-1.19	3419	2.06	3.23
C20b				1.804	5.56	0.907	4.49							
C21a	3342	1.706	0.867	1.794	5.16	0.899	3.58	3339	-0.09	3301	-1.23	3406	1.91	3.18
C21b				1.768	3.63	0.886	-0.11							

TABLE IV. TENSION FORCE OF THE CABLE USING EFFECTIVE LENGTH AND FREQUENCY FROM FINITE ELEMENT METHOD

Cable	T_0	T_2 caluclated from ℓ	T_2^*/T_0	T_2 calulcated from L_1	T_2/T_0	$\frac{\Delta T = T_2^* - T_2}{T_0}$	Due to equation	Due to other factors
	(kN)	(kN)	(%)	(kN)	(%)	(%)	(%)	(%)
C20a	3352	4145	23.66	3641	8.62	15.04	-1.13	9.75
C20b		4191	25.04	3682	9.84	15.04		11.13
C21a	3342	4145	24.03	3641	8.62	15.04	-1.14	10.13
C21b		4026	20.47	3536	5.81	15.04		6.57

TABLE V. CABLE FORE RESULTS USING VIBRATION METHOD ($\overline{T}_1^{07}$) AND MEASUREMENT (T_0) IN 2007

Cable	**C10a**	**C10b**	**C11a**	**C11b**	**C30a**	**C30b**	**C31a**	**C31b**	**Cable**		**C1a**	**C1b**	**C14a**	**C14b**
T_0 (kN)	1470	1458	1406	1426	1426	1406	1426	1406	T_0 (kN)		3635	3632	2057	2057
$\overline{T}_1^{07}$ (kN)	1443	1437	1238	1284	1289	1329	1289	1329	$\overline{T}_2^{07}$ (kN)		4118	4009	1879	1889
$\frac{\overline{T}_1^{07}}{T_0}$ (%)	-1.84	-1.44	-11.95	-9.95	-9.61	-5.46	-9.61	-5.46	$\frac{\overline{T}_2^{07}}{T_0}$ (%)		13.28	10.37	-8.65	-8.17
Cable	**C17a**	**C17b**	**C20a**	**C20b**	**C21a**	**C21b**	**C27a**	**C27b**	**C34a**	**C34b**	**C37a**	**C37b**	**C40a**	**C40b**
T_0 (kN)	2638	2638	3352	3352	3342	3342	2059	2059	2069	2082	2678	2692	3632	3635
$\overline{T}_2^{07}$ (kN)	2942	2884	3641	3682	3641	3536	1976	1972	2341	2320	2821	2836	3836	3812
$\frac{\overline{T}_2^{07}}{T_0}$ (%)	11.52	9.32	8.62	9.85	8.95	5.80	-4.03	-4.22	13.15	11.43	5.34	5.35	5.62	4.69

TABLE VI. EFFECTIVE LENGTH OF BINH BRIDGE CABLE

Cable		ℓ	***SLG***	***SLT***	L_1	**Cable**		ℓ	***SLG***	***SLT***	L_1
Upstream tower	**Downstream tower**					**Upstream tower**	**Downstream tower**				
-	-	(m)	(m)	(m)	(m)	-	-	(m)	(m)	(m)	(m)
C1a/C1b	C40a/C40b	126.964	7.647	2.000	117.317	-	C22a/C22b	126.263	6.013	1.978	118.272
C4a/C4b	C37a/C37b	108.012	6.877	2.020	99.115	-	C23a/C23b	115.264	5.610	2.020	107.634
C7a/C7b	C34a/C34b	77.405	5.302	2.425	69.678	-	C25a/C25b	93.928	4.798	2.190	86.940
C10a/C10b	C31a/C31b	54.180	4.400	4.900	44.880	-	C28a/C28b	65.461	3.625	2.675	59.161
C11a/C11b	C30a/C30b	52.273	4.300	4.795	43.178	-	C29a/C29b	57.748	3.314	3.215	51.219
C14a/C14b	C27a/C27b	74.396	3.980	2.325	68.091						
C17a/C17b	C24a/C24b	104.501	5.213	2.023	97.265						
C20a/C20b	C21a/C21b	137.420	6.045	1.980	129.035						

TABLE VII. TECHNICAL PARAMETERS FOR CALCULATING CABLE TENSION FORCE

Cable	***EA*** **(×10^3)**	***EI***	***w***	L_1	θ	T_0	δ	***C***	ξ	Γ
	(kN)	(kN.m^2)	(kN/m)	(m)	(deg)	(kN)	(m)	-	-	-
C1a/C1b	1817	1930	0.773	117.317	31^{0}39’07"	3635/3632	0.424/0.425	0.0114	161/161	0.001/0.001
C4a/C4b	1411	924	0.602	99.115	35^{0}29’13"	2692/2678	0.323/0.324	0.0181	169/169	0.005/0.005
C7a/C7b	913	375	0.394	69.678	48^{0}11’56"	2082/2069	0.140/0.141	0.0199	164/164	0.003/0.003
C10a/C10b	686	228	0.301	44.880	73^{0}19’01"	1470/1458	0.074/0.075	0.0468	114/113	0.456/0.455
C11a/C11b	641	172	0.279	43.178	72^{0}42’01"	1406/1426	0.067/0.067	0.0416	123/124	0.472/0.472
C14a/C14b	958	457	0.418	68.091	45^{0}00’18"	2057/2057	0.135/0.135	0.0225	144/144	0.024/0.024
C17a/C17b	1229	817	0.530	97.265	32^{0}45’36"	2638/2638	0.268/0.268	0.0130	174/174	0.007/0.007
C20a/C20b	1592	1683	0.684	129.035	25^{0}30’22"	3352/3352	0.477/0.477	0.0093	182/182	0.003/0.003
C21a/C21b	1592	1683	0.684	129.035	25^{0}30’22"	3342/3342	0.478/0.478	0.0093	182/182	0.003/0.003
C22a/C22b	1501	1125	0.643	118.272	27^{0}31’19"	3185/3185	0.398/0.398	0.0094	199/199	0.003/0.003
C23a/C23b	1411	932	0.602	107.634	29^{0}54’22"	2875/2875	0.347/0.347	0.0106	189/189	0.004/0.004
C24a/C24b	1229	817	0.530	97.265	32^{0}45’36"	2639/2639	0.271/0.271	0.0130	174/174	0.007/0.007
C25a/C25b	1139	734	0.490	86.940	36^{0}14’42"	2467/2467	0.217/0.217	0.0160	159/159	0.009/0.009
C27a/C27b	958	457	0.418	68.091	45^{0}00’18"	2059/2059	0.136/0.136	0.0225	144/144	0.024/0.024
C28a/C28b	913	375	0.394	59.161	52^{0}33’46"	1788/1788	0.117/0.117	0.0276	129/129	0.039/0.039
C29a/C29b	821	318	0.355	51.219	61^{0}40’37"	1574/1574	0.094/0.094	0.0357	114/114	0.093/0.093
C30a/C30b	641	172	0.279	43.178	72^{0}42’01"	1426/1406	0.067/0.067	0.0416	124/23	0.472/0.472
C31a/C31b	686	228	0.301	44.880	73^{0}19’01"	1458/1470	0.075/0.074	0.0468	113/114	0.456/0.455
C34a/C34b	913	375	0.394	69.678	48^{0}11’56"	2069/2082	0.141/0.140	0.0199	164/164	0.003/0.003
C37a/C37b	1411	924	0.602	99.115	35^{0}29’13"	2678/2692	0.324/0.323	0.0181	169/169	0.005/0.005
C40a/C40b	1817	1930	0.773	117.317	31^{0}39’07"	3632/3635	0.425/0.424	0.0114	161/161	0.001/0.001

IV. DISCUSSION

The data collected in Table V show that the tension force in the cable at the time of frequency measurement, in addition to the T_0 force component, is also supplemented by the oscillation of the bridge deck girder system under the effects of wind, temperature, etc. The tension force tends to increase at the edge wires and mid-span wires, and vice versa, it tends to decrease for the wires near the tower, reflecting the deformation pattern due to the oscillation of the continuous bridge deck girder system. The deviation level of the tension component is difficult to be determined because it depends on temperature, wind speed, and the deformation of the bridge deck girder or bridge tower at the time of measurement. Based on the data in Table V, it is possible to estimate the additional tension value in the range from -9.95% to 13.18% compared to the initial tension (T_0).

A. Determining the Input Parameters used to Evaluate the Cable Tension of Binh Bridge

Based on the actual structure of the shock absorber of the

stay cables of Binh bridge, the effective length of the cable L_1 was determined according to (18) and the results are summarized in Table VI. The parameter Γ of each stay cable was calculated according to (16) and its shown in Table VII. Table VI shows that all cables have $\Gamma \leq 3$ and $\xi \geq 60$ which are suitable for applying (7). For deeper discussion on cable tension force, the cable was divided into three main groups:

- Group I includes four of the shortest wire pairs at the position closest to the tower pillar are C10a/C10b, C11a/C11b, C30a/C30b, and C31a/C31b with parameters $\Gamma \leq 3$ and $\xi \geq 60$ suitable for calculating cable tension according to (7) when using natural oscillation frequency according to the second oscillation mode f_2 or 13 when using natural oscillation frequency according to the first oscillation mode f_1.
- Group II includes the longest stay cables and some stay cables in intermediate positions: C1a/C1b, C4a/C4b, C7a/C7b, C14a/C14b, C17a/C17b, C20a/C20b, C21a/C21b, C24a/C24b, C27a/C27b, C34a/C34b, C37a/C37b, C40a/C40b with $\Gamma \leq 3$ and $\xi \geq 60$ suitable for calculating the cable force according to (7) and using natural oscillation frequency according to the second oscillation mode f_2.
- Group III includes the stay cables near the bridge girder location that suffered damage due to collision, which were additionally measured after the accident occurred, including the following pairs of cables: C22a/C22b, C23a/C23b, C25a/C25b, C28a/C28b, and C29a/C29b, with $\Gamma \leq 3$ and $\xi \geq 60$, suitable for calculating cable force according to (7).

B. Establishing a Database of Tension in the Cables

1) Vibration Eequipment used from 2015 to 2019

To measure the cable vibration, accelerometers were used. The sensors were verified and the accuracy was guaranteed. The time the measurements were taken ranged between 7 a.m. and 10 a.m. to eliminate the temperature load and the vehicle load effect. The temperature was between 20 ^{0}C and 30 ^{0}C and the wind velocity was between 7 m/s and 14 m/s. The vibration equipment (Figure 5) is listed below:

- Servo acceleration Transducers ASQ-D, with frequency arrangement between 0-300 Hz.
- Sigal Conditioner Dedicated to ASQ: VAG 700A
- PULSE Multi–Analyzer System, Series 3560C
- PULSE 10. 3 analysis software
- Polytec Laser-PDV-100 accelerometers, Series 5015991, frequency arrangement between 0 and 22 KHz

(a) (b) (c)

Fig. 5. Anchor and damper at Binh bridge. (a) Multi–analyzer system, (b) temperature sensor, (c) accelerometer.

2) Determining the Natural Frequencies of the Cable

Fast Fourier Transportation (FFT) was chosen to analyze the natural frequency from the vibration data. The diagonal cables are excited to oscillate by pulling the cable. The first mode natural frequency can be checked by:

$$\overline{f_1} = \frac{\sum_{i=1}^{n-1}(f_{i+1} - f_i)}{n-1} \quad (1)$$

where f_1 , f_i ,.. f_n represent the natural frequencies corresponding to mode $1,i,..n$ and $\overline{f_1}$: is the average natural frequency of mode 1. The natural frequency used in the practical formula is the most suitable $\overline{f_1}$ of one cable in the same stage.

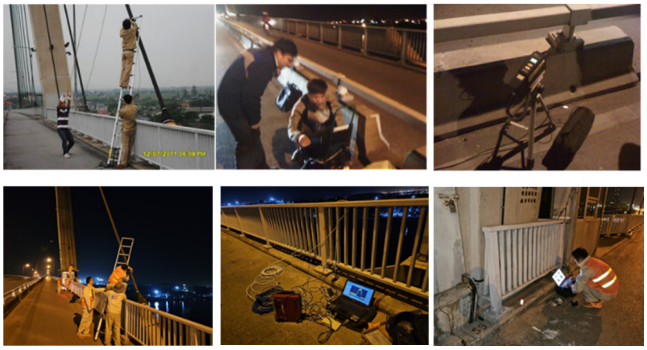

Fig. 6. Cable vibration measurement at Binh Bridge in 2011 and 2023

3) Vibration Monitoring Data of the Bridge's Diagonal Cables through Inspection and Load

The data set on the results of vibration measurement and tension calculation in the cables of Binh bridge during the bridge operation period from 2005 to 2019 and 2023 is summarized in Table VIII. Figure 6 displays several vibration measurement activities that occurred onsite during this period. In some cases the natural vibration frequencies corresponding to the first and second vibration modes cannot be detected because the measurement process at the bridge site is often affected by many factors [6, 16]. The vibration measurement data in 2010 and 2011 were tested in a damaged bridge, operating under load restriction mode. Figure 7 shows the acceleration graph in frequency form of some cables of Binh bridge obtained from the inspection in 2009, 2010, and 2019 used to determine the natural frequency according to (20). The data were collected into 3 stages:

Stage 1: From 2005 to 2009, regular monitoring process before the incident of the ship collision with the main girder. Only 4 stay cables were inspected in 2005 because the bridge was newly built. From 2007 to 2009, 32 stay cables were inspected annually.

Stage 2: From 2010 to 2012, measurements were made during temporary operation and troubleshooting. During this period, 10 additional cables were measured each year in the area along the bridge near the ship collision site, including

additional measurements of diagonal cables numbered: C22a, C22b, C23a, C23b, C25a, C25b, C28a, C28b, C29a and C29b (Table VI). A total of 42 cables were measured for oscillation frequency.

Stage 3: After completing the bridge repair and post-repair inspection (2012), continuous monitoring equipment was installed at some essential locations, using data from the continuous monitoring system. However, because the continuous monitoring system was not working completely stably, in 2019 and 2023, inspections were conducted on 42 stay cables as was done from 2010 to 2012.

Binh Bridge in Hai Phong - Vietnam can be considered a special case because it has been periodically inspected the most times (9 times/19 years) among the cable-stayed bridges built in Vietnam. All inspections were conducted by the Vietnam University of Transport, the data set was accumulated over 19 years from 2005 to 2019 and in 2023, in addition to the purpose of assessing the technical status and ensuring the safe operation of the bridge, they are also experimental data serving the purpose of studying the tension force in the cable-stayed cables on the actual bridge model.

TABLE VIII. DATA SET OF VIBRATION MEASUREMENT RESULTS OF CALCULATING THE TENSION FORCE FOR THE STAY CABLES OF THE BINH BRIDGE FROM 2005 TO 2019 AND 2023

Dataset Label	Time	Number of cables	Cables	Number of measurements for 1 cable	Number of frequeniesy for 1 cable	Total
CB-2005	06/4/2005	4	C20a, C20b, C21a, C21b	3	4	12
CB-2007	28/10/2007	32	C1a, C1b, C4a, C4b, C7a, C7b, C10a, C10b, C11a, C11b, C14a, C14b, C17a, C17b, C20a, C20b, C21a, C21b, C24a, C24b, C27a, C27b, C30a, C30b, C31a, C31b, C34a, C34b, C37a, C37b, C40a, C40b	3	6	32×18
CB-2008	10/9/2008			3	6	32×18
CB-2009	06/9/2009			3	6	32×18
CB-2010	19/7/2010	42	C1a, C1b, C4a, C4b, C7a, C7b, C10a, C10b, C11a, C11b, C14a, C14b, C17a, C17b, C20a, C20b, C21a, C21b, C22a, C22b, C23a, C23b, C24a, 24b, C25a, C25b, C27a, C27b, C28a, C28b, C29a, C29b, C30a, C30b, C31a, C31b, C34., C34b, C37a, C37b, C40a, C40b	3	6	42×18
CB-2011	12/2/2011			3	6	42×18
CB-2012	16/11/2012			3	6	42×18
CB-2023	06/12/2023			3	6	42×18
CB-2019	23/11/2019	32	C1a, C1b, C4a, C4b, C7a, C7b, C10a, C10b, C11a, C11b, C14a, C14b, C17a, C17b, C20a, C20b, C21a, C21b, C24a, C24b, C27a, C27b, C30a, C30b, C31a, C31b, C34a, C34b, C37a, C37b, C40a, C40b	3	6	32×18

C. Analysis of the Tension Force in the Diagonal Cables

Based on cable figuration, (15) is used to calculate C and (4) to (13) are selected to estimate the tension force T. Table IX and Table X present the frequency f_1 (f_2) and tension T_1 (T_2) of 4 pairs of stay cables belonging to group I from 2007 to 2023 (17 years). The differences of measurement frequency data of each year with the year 2007 is presented. Table XI shows the largest annual average value of the change in oscillation frequency f_1 (f_2) and tension T_1 (T_2) of the cables belonging to group I. Table XII and Table XIII show the changes in frequency f_2 and tension T_2 calculated by (7) of the stay cables from 2007 to 2023 of 12 stay cable pairs belonging to group II. Table XIV shows the maximum annual average value of the change in frequency f_2 and tension T_2 of the 4 pairs of longest stay cables in group II after 17 years of operation (from 2007 to 2023). Table XV shows the changes in frequency f_2 and tension of 5 cable pairs belonging to group III that were additionally measured and tested after the ship collision with structural parameter $\Gamma < 3$. Since this group does not have measurement data in 2007, the changes in tension of the measurements are compared with the initial tension T_0. Figures 8 to 12 show the change in tension determined by the oscillation method of the 10 most important pairs of diagonal cables, including 2 pairs of anchor cables (C1a, C1b, and C40a, C40b); 2 longest pairs of cables in the main span (C20a, C20b, and C21a, C21b); 2 intermediate pairs of cables, including 1 pair of cables in the main girder area damaged by ship collision (C24a, C24b) and 1 pair of cables symmetrical to the damaged area (C14a, C14b); 2 pairs of cables close to the tower pillar on the Hai Phong side (C10a, C10b, and C11a, C11b) and 2 pairs of cables close to the tower pillar on the Thuy Nguyen side (C30a, C30b, and C31a, C31b). The results of the long-term monitoring series with 8 times/19 years of measuring cable tension of Binh bridge by the vibration method presented in Tables IX to XV allow the following discussions and comments.

- Regarding the suitability of the vibration behavior of cable-stayed cables

The monitoring data series is systematic and contains a sufficient quantity of data. No abnormal data were detected between measurements, except for the data in 2010 and 2011 due to the incident. This reflects the reliability of the method of determining tension by vibration measurement. When an incident occurs, the change in tension in the cables is consistent with the damaged state of the structure. The long-term monitoring data spanning 17 years of operation (2017 - 2023) of the cable-stayed system of Binh Bridge indicates a consistent decrease in tension. The largest decrease for cables in group I is -8.06% (average decrease of -0.474% per year); for group II, it is -9.44% (-0.555% average per year); and for group III (following repairs in 2012), it is -3.93% with an average decrease of -0.328% per year. The observed phenomenon aligns with mechanical principles, as manifested by the slackening of steel cables, decreased height of the bridge tower due to creep, and an increase in the inelastic deflection of the bridge deck girder system.

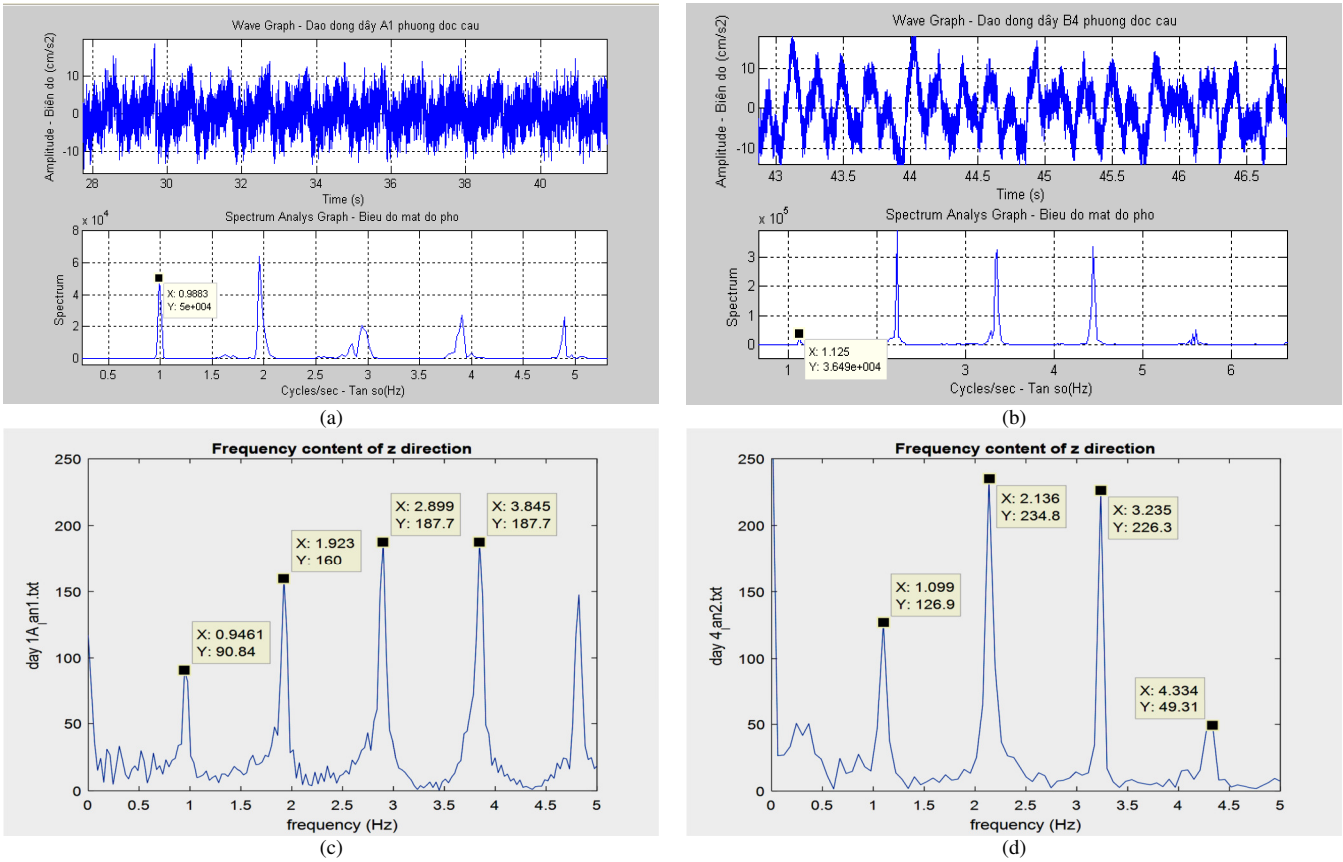

Fig. 7. Accelerometers and frequency data of bridge cables in 2009 and 2019. (a) Cable C1a, 2009, (b) cable C4b, 2009, (c) cable C1a, 2019, (d) cable C4b, 2019.

TABLE IX. SURVEY RESULTS OF CHANGES IN NATURAL FREQUENCY IN GROUP I FROM 2007 TO 2023

Cable	2007	2008		2009		2010		2011		2012		2019		2023	
	$\bar{f}_1^{07}$ ($\bar{f}_2^{07}$)	$\bar{f}_1^{08}$ ($\bar{f}_2^{08}$)	Diff	$\bar{f}_1^{09}$ ($\bar{f}_2^{09}$)	Diff	$\bar{f}_1^{10}$ ($\bar{f}_2^{10}$)	Diff	$\bar{f}_1^{11}$ ($\bar{f}_2^{11}$)	Diff	$\bar{f}_1^{12}$ ($\bar{f}_2^{12}$)	Diff	$\bar{f}_1^{19}$ ($\bar{f}_2^{19}$)	Diff	$\bar{f}_1^{23}$ ($\bar{f}_2^{23}$)	Diff
	(Hz)	(Hz)	(%)	(Hz)	(%)	(Hz)	(%)								
C10a	2.468	2.463	-0.20	2.448	-0.81	2.478	0.41	2.438	-1.22	-	-	2.442	-1.05	2.368	-4.05
	(4.973)	(4.914)	(-1.19)	(4.947)	(-0.51)	(5.030)	(1.15)	(4.900)	(-1,46)	-	-	(4.860)	(-2.27)	(4.795)	(-3.57)
C10b	2.432	2.438	0.25	2.411	-0.86	2.489	2.34	2.469	1.52	-	-	2.438	0.25	2.356	-3.13
	(4.922)	(4.934)	(0.25)	(4.846)	(-1.54)	(5.052)	(2.65)	(5.024)	(2.08)	-	-	(4.863)	(-1.18)	(4.700)	(-4.51)
C11a	2.462	2.433	-1.18	2.448	-0.57	2.402	-2.44	2.375	-3.53	-	-	2.425	-1.50	2.388	-3.00
	(4.968)	(5.008)	(0.81)	(4.884)	(-1.69)	(4.880)	(-1.77)	(4.807)	(-3.24)	-	-	(4.896)	(-1.45)	(4.776)	(-3.86)
C11b	2.507	2.486	-0.84	2.481	-1.04	2.421	-3.43	2.397	-4,38	-	-	2.442	-2.59	2.452	-2.19
	(5.050)	(5.006)	(-1.76)	(4.978)	(-1.43)	(4.878)	(-4.21)	(4.846)	(-4.04)	-	-	(4.952)	(-1.94)	(4.899)	(-2.99)
C30a	2.512	2.475	-1.47	2.499	-0.05	2.490	-0.08	2.452	-2.39	2.461	-2,03	2.463	-1.95	2.408	-4.14
	(5.048)	(5.002)	(-0.91)	(4.986)	(-1.23)	(5.014)	(-0.67)	(4.950)	(-1.94)	(4.946)	(-2.02)	(4.938)	(-2.18)	(4.840)	(-4.12)
C30b	2.550	2.513	-1.45	2.498	-2.04	2.471	-3.10	2.520	-1.18	2.477	-2.86	2.503	-1.84	2.460	-3.53
	(5.092)	(5.038)	(-1.06)	(5.030)	(-1.22)	(4.982)	(-2.16)	(5.006)	(-1.69)	(4.950)	(-2.79)	(4.994)	(-1.92)	(4.920)	(-3.38)
C31a	2.601	2.600	-0.04	2.573	-1.08	2.538	-2.42	2.580	-0.81	2.578	-0.88	2.625	0.92	2.528	-2.81
	(5.238)	(5.184)	(-1.02)	(5.140)	(-1.87)	(5.056)	(-3.48)	(5.134)	(-1.99)	(5.134)	(-1.99)	(5.200)	(-0.73)	(5.040)	(-3.78)
C31b	2.628	2.625	-0.11	2.624	-0.15	2.546	-3.12	2.609	-0.72	2.607	-0.80	2.625	-0.11	2.558	-2.66
	(5.192)	(5.240)	(0.92)	(5.090)	(-1.96)	(5.080)	(-2.16)	(5.144)	(-0.92)	(5.200)	(0.15)	(5.104)	(-1.69)	(5.073)	(-2.19)

Note: (-) no measurement data, Diff: Differences

TABLE X. SURVEY RESULTS OF CHANGES IN TENSION FORCE IN GROUP I FROM 2007 TO 2023

Cable	Applied Equation	2007	2008		2009		2010		2011		2012		2019		2023	
		$\overline{T}_1^{07}$	$\overline{T}_1^{08}$	Diff	$\overline{T}_1^{09}$	Diff	$\overline{T}_1^{10}$	Diff	$\overline{T}_1^{11}$	Diff	$\overline{T}_1^{12}$	Diff	$\overline{T}_1^{19}$	Diff	$\overline{T}_1^{23}$	Diff $\overline{T}_1^{07}$
		(kN)	(kN)	(%)	(Hz)	(%)	(Hz)	(%)	(kN)	(%)	(Hz)	(%)	(Hz)	(%)	(Hz)	(%)
C10a	(7)	1465	1430	-2.39	1450	-1.04	1499	2.32	1422	-2.94	-	-	1399	-4.50	1361	-7.08
	(13)	1442	1436	-0.42	1419	-1.59	1454	0.83	1407	-2.42	-	-	1412	-2.08	1327	-7.97
C10b	(7)	1434	1441	0.49	1390	-3.07	1510	5.29	1494	4.18	-	-	1400	-2.37	1307	-8.83
	(13)	1399	1406	0.49	1375	-1.72	1465	4.72	1442	3.07	-	-	1406	0.49	1313	-6.15
C11a	(7)	1260	1280	1.16	1218	-3.33	1216	-3.49	1180	-6.36	-	-	1224	-2.86	1165	-7.53
	(13)	1237	1209	-2.26	1223	-1.13	1177	-4.85	1151	-6.94	-	-	1200	-2.98	1164	-5.90
C11b	(7)	1302	1279	-1.77	1265	-2.84	1215	-6.68	1200	-7,83	-	-	1252	-3.82	1225	-5.88
	(13)	1284	1262	-1.69	1257	-2.10	1197	-6.78	1174	-8.57	-	-	1218	-5.14	1228	-4.36
C30a	(7)	1301	1277	-1.81	1270	-2.38	1284	-1.31	1251	-3.84	1249	-3,99	1245	-4.30	1197	-7.99
	(13)	1289	1251	-2.92	1276	-1.01	1267	-1.71	1228	-4.72	1237	-4.03	1239	-3.86	1185	-8.06
C30b	(7)	1325	1297	-2.11	1292	-2.46	1268	-4.28	1280	-3.35	1252	-5.51	1275	-3.77	1237	-6.64
	(13)	1329	1291	-2.86	1275	-4.06	1248	-6.10	1298	-2.33	1254	- 5.64	1281	-3.61	1237	-6.92
C31a	(7)	1555	1525	-1.93	1498	-3.67	1451	-6.68	1495	-3.86	1495	-3.86	1533	-1.39	1441	-7.33
	(13)	1534	1533	-0.07	1501	-2.15	1461	-4.76	1509	-1.63	1507	-1.76	1562	1.83	1449	-5.54
C31b	(7)	1600	1630	1.88	1538	-3.87	1539	-6.16	1532	-4.25	1605	-0.31	1546	-3.37	1493	-6.69
	(13)	1639	1636	-0.18	1634	-0.31	1538	-6.16	1615	-1.46	1613	-1.59	1635	-0.24	1553	-5.25

TABLE XI. MAXIMUM ANNUAL AVERAGE CHANGE OF FREQUENCY f_1 (f_2) AND TENSION T_1 (T_2) OF GROUP I CABLES FROM 2007 TO 2023

Cable	C10a	C10b	C11a	C11b	C30a	C30b	C31a	C31b
f_1	-0.238	-0.265	-0.227	-0.176	-0.244	-0.208	-0.199	-0.157
T_1	-0.469	-0.519	-0.443	-0.346	-0.474	-0.407	-0.431	-0.394

TABLE XII. SURVEY RESULTS OF CHANGES IN NATURAL FREQUENCY f_2 IN GROUP II STAY CABLES FROM 2007 TO 2023

Cable	2007	2008		2009		2010		2011		2012		2019		2023	
	$\overline{f}_2^{07}$	$\overline{f}_2^{08}$	Diff	$\overline{f}_2^{09}$	Diff	$\overline{f}_2^{10}$	Diff	$\overline{f}_2^{11}$	Diff	$\overline{f}_2^{12}$	Diff	$\overline{f}_2^{19}$	Diff	$\overline{f}_2^{23}$	Diff
	(Hz)	(Hz)	(%)	(Hz)	(%)	(Hz)	(%)	(Hz)	(%)	(Hz)	(%)	(Hz)	(%)	(Hz)	(%)
C1a	1.974	1.956	-0.91	1.976	0.10	1.987	0.66	1.972	0.10	-	-	1.923	-2.58	1.880	-4.76
C1b	1.948	1.946	-0.10	1.952	0.21	1.906	-2.16	1.936	-0.62	-	-	1.916	-1.64	1.900	-2.46
C4a	2.166	2.154	-0.06	2.188	1.02	2.176	0.46	2.190	1.11	-	-	2.196	1.39	2.136	-1.39
C4b	2.208	2.226	0.82	2.251	1.95	2.410	9.14	2.397	8.56	-	-	2.136	-3.43	2.138	-3.17
C7a	3.588	3.600	-0.33	3.499	-2.48	3.632	1.23	3.500	-2.45	-	-	3.540	-1.34	3.488	-3.79
C7b	3.558	3.556	-0.06	3.604	1.29	3.578	0.56	3.562	0.61	-	-	3.558	0.00	3.502	-1.63
C14a	3.134	3.116	-0.57	3.154	0.64	3.128	-0.19	3.126	-0.26	3.116	-0.57	3.106	-0.89	3.048	-2.74
C14b	3.142	3.142	0.00	3.154	0.38	3.140	-0.06	3.126	-0.51	3.100	-1.34	3.072	-2.23	3.068	-2.36
C17a	2.428	2.426	-0.08	2.480	2.14	2.432	0.17	2.436	0.33	2.422	-0.25	2.426	-0.08	2.368	-2.47
C17b	2.404	2.406	0.08	2.460	2.33	2.456	2.16	2.438	1.41	2.400	-0.17	2.396	-0.33	2.342	-2.58
C20a	1.794	1.784	-0.56	1.818	1.34	1.792	0.11	1.812	1.00	1.802	0.45	1.784	-0.56	1.782	-0.67
C20b	1.804	1.830	1.44	1.822	1.00	1.794	-0.55	1.812	0.44	1.832	1.55	1.830	1.44	1.820	0.89
C21a	1.794	1.790	-0.22	1.774	-1.12	1.870	4.24	1.860	3.68	1.806	0.67	1.792	-0.11	1.772	-1.23
C21.b	1.768	1.768	0.00	1.772	0.23	1.796	1.68	1.802	1.92	1.770	0.11	1.770	0.11	1.768	0.00
C24a	2.440	2.440	0.00	2.430	-0.41	2.462	0.90	2.448	0.33	2.424	-0.66	2.404	-1.48	2.372	-2.78
C24b	2.418	2.422	0.17	2.440	2.15	2.486	2.81	2.452	1.41	2.446	1.16	2.404	-0.58	2.386	-1.32
C27a	3.212	3.214	0.06	3.216	0.12	3.256	1.37	3.266	1.68	3.216	0.13	3.214	0.06	3.162	-1.56
C27b	3.208	3.228	0.62	3.238	0.94	3.258	1.56	3.272	2.00	3.224	0.50	3.216	0.25	3.184	-0.74
C34a	3.504	3.508	-0.11	3.544	1.14	3.532	0.80	3.562	1.66	-	-	3.500	-0.11	3.480	-1.26
C34b	3.488	3.484	0.12	3.442	-1.32	3.516	0.80	3.526	1.09	-	-	3.488	0.00	3.466	-0.63
C37a	2.202	2.196	-0.27	2.204	0.09	2.242	1.82	2.212	0.45	-	-	2.158	-2.00	2.150	-2.36
C37b	2.208	2.190	-0.82	2.204	0.18	2.272	2.89	2.252	1.99	-	-	2.168	1.81	2.152	-2.54
C40a	1.906	1.920	0.74	1.942	1.90	1.938	1.68	1.936	1.57	-	-	1.892	-0.75	1.827	-4.14
C40b	1.900	1.892	-0.42	1.916	0.84	1.948	2.52	1.936	1.90	-	-	1.892	-0.42	1.808	-4.84

TABLE XIII. SURVEY RESULTS OF CHANGES IN TENSION FORCE IN GROUP II CALCLUATED BASED ON f_2 FROM 2007 TO 2023

Cable	2007	2008		2009		2010		2011		2012		2019		2023	
	$\overline{T}_2^{07}$	$\overline{T}_2^{08}$	Diff	$\overline{T}_2^{09}$	Diff	$\overline{T}_2^{10}$	Diff	$\overline{T}_2^{11}$	Diff	$\overline{T}_2^{12}$	Diff	$\overline{T}_2^{19}$	Diff	$\overline{T}_2^{23}$	Diff
	(Hz)	(Hz)	(%)	(Hz)	(%)	(Hz)	(%)	(Hz)	(%)	(Hz)	(%)	(Hz)	(%)	(Hz)	(%)
C1a	4118	4043	-1.82	4126	1.94	4172	1.31	4110	-0.19	-	-	3908	-5.10	3735	-9.30
C1b	4009	4001	-0.20	4026	0.42	3838	4.26	3960	-1.22	-	-	3878	-3.27	3814	-4.86
C4a	2724	2693	-1.14	2780	2.06	2748	0.88	2784	2.20	-	-	2780	2.06	2649	-2.75
C4b	2896	2943	1.62	3010	3.94	3450	19.14	3413	17.85	-	-	2710	-6.41	2625	-9.36
C7a	2449	2465	0.65	2328	-4.94	2509	2.50	2330	-4.86	-	-	2389	-2.45	2314	-5.55
C7b	2407	2404	-0.12	2469	2.57	2434	1.12	2413	0.25	-	-	2407	0.00	2332	-3.12
C14a	1879	1858	-1.12	1903	1.28	1872	0.37	1869	-0.53	1858	-1.11	1846	-1.11	1777	-5.43
C14b	1889	1889	0.00	1903	0.74	1886	0.16	1869	-1.06	1838	-2.70	1806	-4.41	1801	-4.66
C17a	2942	2937	-0.17	3069	4.31	2952	0.34	2961	0.64	2927	-0.51	2937	-0.17	2798	-4.89
C17b	2884	2888	0.14	3019	4.68	3010	4.37	2966	2.84	2874	-0.35	2864	-0.69	2737	5.10
C20a	3641	3601	-1.10	3739	2.69	3633	-0.22	3714	2.01	3674	0.91	3601	-1.10	3593	-1.32
C20b	3682	3789	2.90	3756	2.01	3641	-1.11	3715	0.90	3797	3.12	3789	2.91	3748	1.79
C21a	3641	3625	-0.44	3560	-2.22	3956	8.65	3914	7.50	3690	1.35	3633	-0.22	3552	-2.44
C21b	3536	3536	0.00	3552	0.45	3649	3.20	3673	3.87	3544	0.27	3544	0.23	3536	0.00
C24a	2985	2985	0.00	2960	-0.84	3039	1.81	3014	0.98	2946	-1.31	2898	-2.92	2821	-5.49
C24b	2887	2878	0.31	2919	1.11	3032	5.03	2950	2.18	2936	1.70	2836	-1.77	2793	-3.26
C27a	1976	1978	0.10	1981	0.25	2030	2.73	2043	3.39	1981	0.25	1978	0.10	1915	-3.09
C27b	1972	1996	1.22	2008	1.83	2033	3.09	2051	4.01	1991	0.96	1981	0.46	1942	-1.52
C34a	2341	2347	0.26	2395	2.31	2379	1.62	2420	3.37	-	-	2336	-0.21	2310	-1.32
C34b	2320	2315	-0.22	2259	-2.63	2358	1.64	2371	2.19	-	-	2320	0.00	2291	-1.25
C37a	2821	2806	-0.53	2826	0.18	2925	3.69	2847	0.92	-	-	2709	-3.97	2640	-4.36
C37b	2836	2689	-0.74	2836	4.69	2745	1.33	2694	-0.54	-	-	2735	-3.56	2694	-5.01
C40a	3836	3893	1.49	3983	3.83	3966	3.39	3958	3.18	-	-	3780	-1.46	3525	-8.10
C40b	3812	3780	-0.84	3877	1.71	4007	5.11	3958	3.83	-	-	3780	-0.84	3452	-9.44

TABLE XIV. MAXIMUM ANNUAL AVERAGE CHANGE OF FREQUENCY f_2 AND TENSION T_2 OF LONGEST CABLE BELONG TO GROUP II FROM 2007 TO 2023

Cable	**C1a**	**C1b**	**C20a**	**C20b**	**C21a**	**C21b**	**C40a**	**C40b**
f_2	-0.280	-0.145	-0.039	0.052	-0.072	0.000	-0.244	-0.285
T_2	-0.547	-0.286	-0.078	0.105	-0.144	0.000	-0.477	-0.555

TABLE XV. SURVEY RESULTS OF CHANGES SECOND MODE FREQUENCY f_2 AND TENSION FORCE OF GROUP III FROM 2010 TO 2023

Cable	T_0	2010			2011			2012			2023				Average annual change
		$\overline{f}_2^{10}$	$\overline{T_2^{10}}$	Difference with T_0	$\overline{f}_2^{11}$	$\overline{T_2^{11}}$	Difference with T_0	$\overline{f}_2^{12}$	$\overline{T_2^{12}}$	Difference with T_0	$\overline{f}_2^{23}$	$\overline{T_2^{23}}$	Difference with T_0	Difference with $\overline{T_2^{12}}$	
	(kN)	(Hz)	(kN)	(%)	(Hz)	(kN)	(%)	(Hz)	(kN)	(%)	(Hz)	(kN)	(%)	(%)	(%)
C22a	3185	2.082	3899	22.42	2.062	3825	20.09	1.962	3463	8.73	1.928	3344	8.13	-0.60	-0.050
C22b	3185	2.008	3627	13.88	2.012	3642	14.35	1.938	3379	6.09	1.908	3315	4.08	-2.10	-0.175
C23a	2875	2.176	3264	13.53	2.164	3228	12.27	2.140	3157	9.80	2.128	3122	8.59	-1.21	-0.100
C23b	2875	2.124	3179	10.57	2.109	3134	9.01	2.102	3114	8.31	2.088	3072	6.86	-1.45	-0.121
C25a	2467	2.620	2520	2.15	2.626	2530	6.45	2.646	2570	4.18	2.618	2515	1.95	-2.23	-0.186
C25b	2467	2.640	2561	3.81	2.626	2534	2.72	2.608	2499	1.30	2.578	2442	-1.01	-2.31	-0.293
C28a	1788	3.818	1984	10.96	3.824	1990	11.30	3.788	1953	9.22	3.746	1910	6.82	-2.40	-0.200
C28b	1788	3.822	1988	11.19	3.816	1982	10.85	3.800	1965	9.90	3.746	1910	6.82	-3.08	-0.257
C29a	1574	4.078	1518	-3.55	4.102	1536	-2.41	4.098	1533	-2.61	3.992	1471	-6.54	-3.93	-0.328
C29b	1574	4.180	1595	1.33	4.062	1506	-4.32	4.096	1532	-2.67	3.996	1474	-6.38	-3.71	-0.309

- Regarding the alteration of force in the cable-stayed cables

The tension in the cables varies depending on the structure and cable position. The anchor cables (C1a, C1b, C40a, and C40b) experienced the largest change in tension, with the greatest decrease occurring in cable C40b (-9.44%). This decrease is attributed to the cables' significant length, small tilt angle, and susceptibility to substantial relaxation (Figure 10). It is important to note that the anchor cables connect to the top of the anchor piers, so they are not affected by the deflection of the bridge deck girder system. The cables at the mid-span position (C20a, C20b, C21a, and C21b) have the same length and angle of inclination as the anchor cable group but experience a much smaller decrease in tension force. The largest decrease in this group is found in cable C21a at -2.44%. This can be explained by the fact that although these cables suffer from the same slack phenomenon as the cables in the anchor cable group, they are also affected by the deflection of the bridge deck girder system, which helps maintain the tension force in the cables with little decrease. The significant attenuation in wire C10b, which has the highest attenuation value at 8.83%, is due to the fact that it, along with wires C10a, C11a, C11b, C30a, C30b, C31a, and C31b, is supported on the bridge bearing. This means that the bridge deck girder system

at the connection point of these wires does not experience any sagging deformation. In a scenario where both ends are connected to the tower and the fixed girder, any slack phenomenon will decrease the tension in the cable without affecting the maintenance of tension force, or the deformation of the bridge deck girder system.

- Regarding the impact of natural frequency on the bridge structural health:

During the period from 2005 to 2009 before the ship collisions, the cable tension remained stable. The frequency change ranged from 0.00% to -3.29%, resulting in cable tension errors ranging from 0.00% to -6.47%. The ship collision caused some damage to the steel girder and tore the sheath of cable 23a. It also led to a significant change in the tension of some cables, but the damage only affected a specific area. The incident altered the frequency and tension of some stay cables in groups II and III. The most notable changes measured in 2010 were the following: cable C14b tension increased by 19.14% compared to its original value $\overline{T}_2^{07}$ (a 28.83% increase compared to T_0); cable C22a increased by 22.42% compared to its initial tension T_0; and cable C21a increased by 8.65% compared to its tension $\overline{T}_2^{07}$ (an 18.37% increase compared to T_0). The survey revealed that cables 23a and 24a had torn sheaths, resulting in a significant change in tension. In 2010, the tension of cable C23a increased by 13.53% compared to its initial tension T_0, while the tension of cable C24a increased by 1.81% compared to the tension measured in 2007 and by 13.11% compared to T_0. Notably, the increase in tension was less sudden compared to cables located further from the impact area. After repairing the steel beams and re-tensioning the cables in 2012, the stay cables all worked stably, showing no abnormal natural frequencies detected through the test measurements.

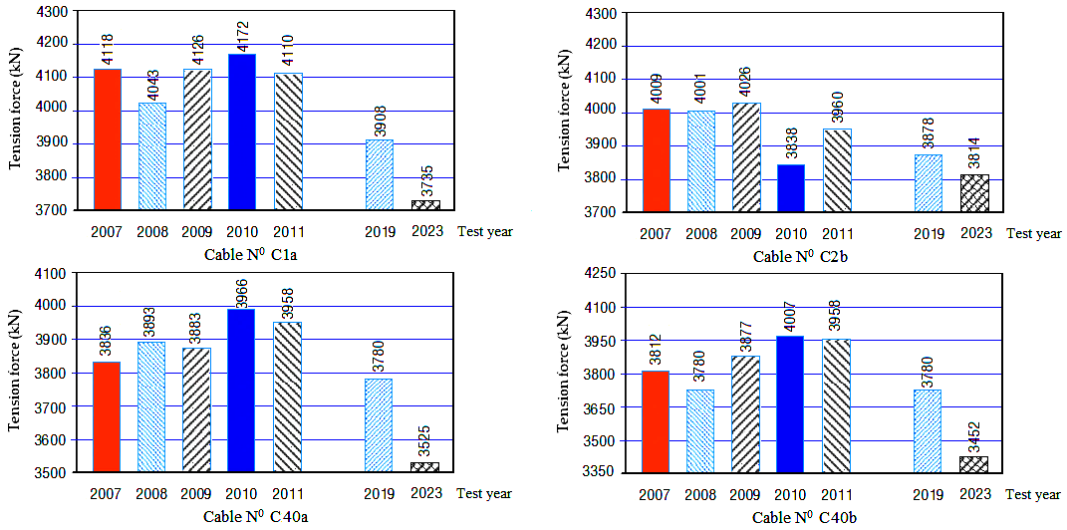

Fig. 8. Tension force changes in cables C1a, C1b, C40a and C40b of Binh bridge from 2007 to 2023.

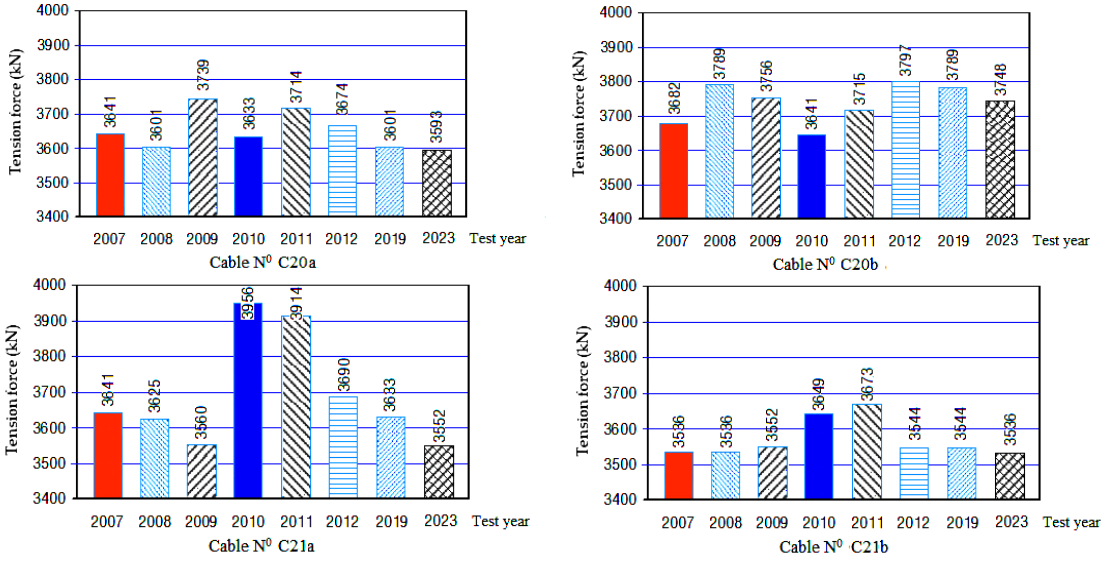

Fig. 9. Tension force changes in cables C20a, C20b, C21a and C21b of Binh bridge from 2007 to 2023.

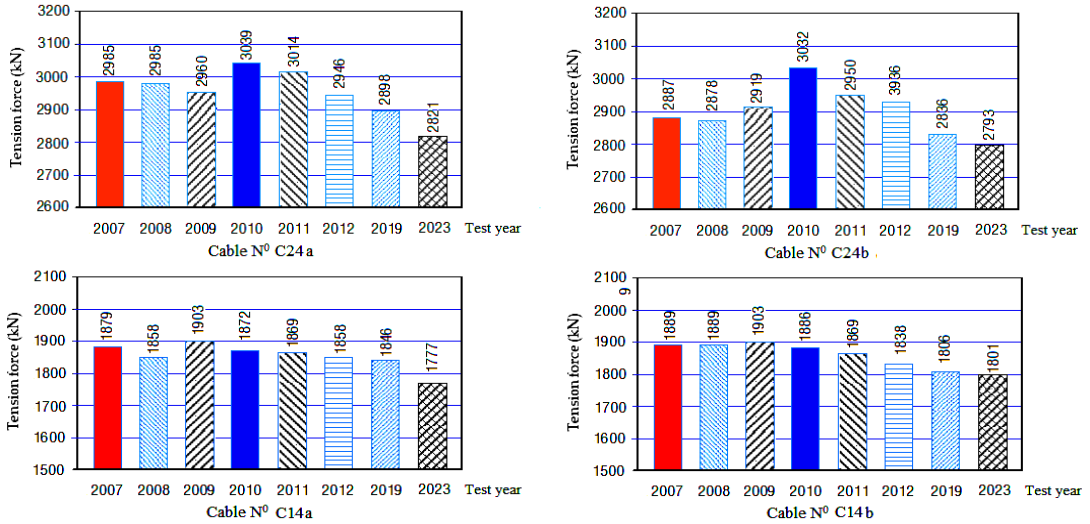

Fig. 10. Tension force changes in cables C24a, C24b, C14a and C14b of Binh bridge from 2007 to 2023.

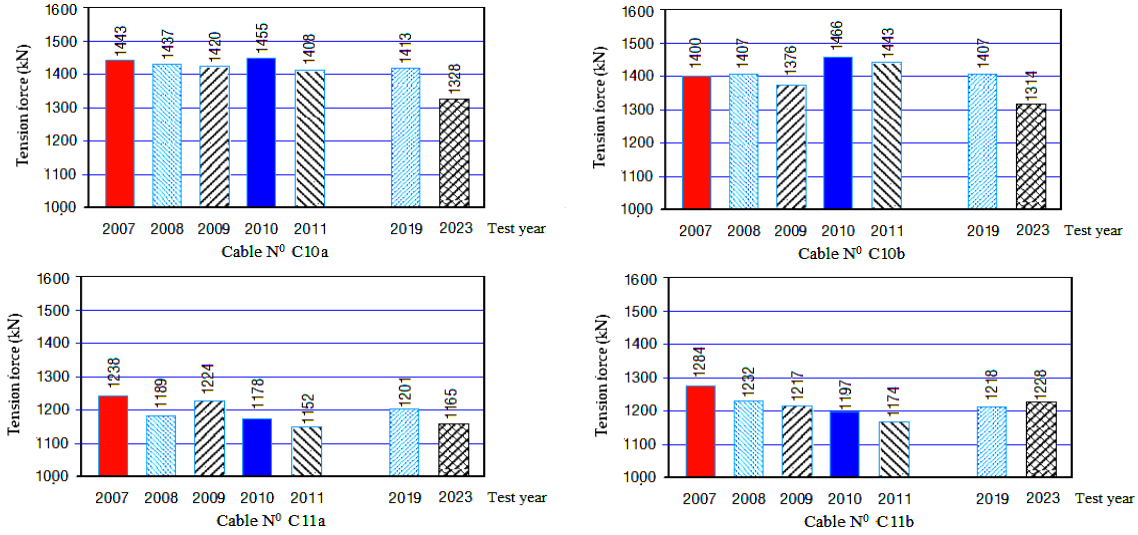

Fig. 11. Tension force changes in cables C10a, C10b, C11a, and C11b of Binh bridge from 2007 to 2023.

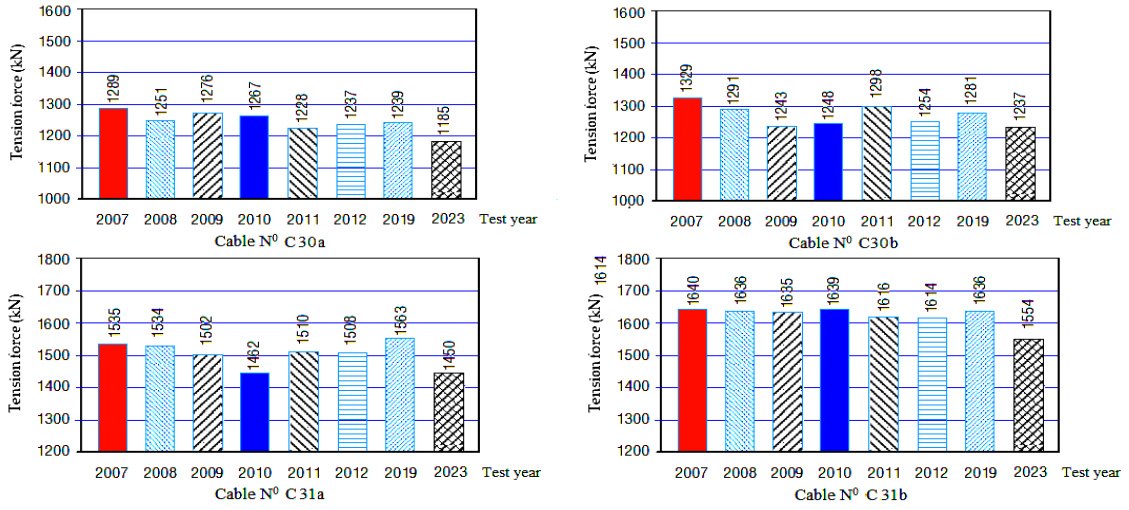

Fig. 12. Tension force changes in cables C30a, C30b, C31a, and C31b of Binh bridge from 2007 to 2023.

V. CONCLUSION

A long-term monitoring program spanning 19 years, from 2005 to 2023, was conducted on Binh Bridge (Hai Phong) in Vietnam, with a specific focus on the 17-year period from 2007 to 2023. The program aimed to monitor changes in the tension of 32 cables included in the official study and of 10 additional cables. The data collected allowed for the assessment of cable tension using the oscillation method, ensuring a reliable level of accuracy.

Considering the effect of damping devices at both ends of the cables on the effective length reduced the error in the tension value by about 15% compared to previous studies. The reliability of these data was confirmed by comparing them with the initial actual tension in the cables stored in the bridge completion records, while separating it from other error-causing factors. It was determined that the remaining deviation in the range of -1.44 to 13.28% was caused by random factors, such as oscillations of the bridge deck girder system, temperature, operation, and measuring equipment. These results can be considered satisfactory under experimental conditions on actual cable-stayed bridges.

The Binh Bridge's cable-stayed system has been operating stably, with no abnormalities detected, except for the 2010 ship collision incident. This incident caused partial damage to the steel girder and affected the tension in some cables, but it was repaired and the bridge has operated without issues since then. The largest decrease in cable-stayed tension was -9.44% (averaging -0.555% per year) after 19 years of operation.

This study highlights the importance of accurately determining the true parameters of the stay cables and utilizing the initial tension storage data when determining the cable tension using the oscillation method during load testing of actual cable-stayed bridges.

ACKNOWLEDGMENT

The research team would like to express their sincere gratitude to the Hai Phong City People's Committee, Hai Phong Bridge Project Management Board, and the University of Transport for providing funding and creating favorable conditions to support the equipment needed to complete this study.

REFERENCES

[1] S. Cho, J. Yim, S. W. Shin, H.-J. Jung, C.-B. Yun, and M. L. Wang, "Comparative Field Study of Cable Tension Measurement for a Cable-Stayed Bridge," *Journal of Bridge Engineering*, vol. 18, no. 8, pp. 748–757, Aug. 2013, https://doi.org/10.1061/(ASCE)BE.1943-5592.0000421.

[2] Y.-F. Duan *et al.*, "Development of Elasto-Magneto-Electric (EME) Sensor for In-Service Cable Force Monitoring," *International Journal of Structural Stability and Dynamics*, vol. 16, no. 4, Mar. 2016, Art. no. 1640016, https://doi.org/10.1142/S0219455416400162.

[3] S. E. Haji Agha Mohammad Zarbaf, M. Norouzi, R. J. Allemang, V. J. Hunt, A. Helmicki, and D. K. Nims, "Stay Force Estimation in Cable-Stayed Bridges Using Stochastic Subspace Identification Methods," *Journal of Bridge Engineering*, vol. 22, no. 9, Sep. 2017, Art. no. 04017055, https://doi.org/10.1061/(ASCE)BE.1943-5592.0001091.

[4] B. H. Kim and T. Park, "Estimation of cable tension force using the frequency-based system identification method," *Journal of Sound and Vibration*, vol. 304, no. 3, pp. 660–676, Jul. 2007, https://doi.org/10.1016/j.jsv.2007.03.012.

[5] Y. Bao, Z. Shi, J. L. Beck, H. Li, and T. Y. Hou, "Identification of time-varying cable tension forces based on adaptive sparse time-frequency analysis of cable vibrations," *Structural Control and Health Monitoring*, vol. 24, no. 3, Mar. 2017, Art. no. e1889, https://doi.org/10.1002/stc.1889.

[6] M.-H. Nguyen, T.-D.-N. Truong, T.-C. Le, and D.-D. Ho, "Identification of Tension Force in Cable Structures Using Vibration-Based and Impedance-Based Methods in Parallel," *Buildings*, vol. 13, no. 8, Aug. 2023, Art. no. 2079, https://doi.org/10.3390/buildings13082079.

[7] H. D. Nguyen, S. Khatir, and Q. B. Nguyen, "A Novel Method for the Estimation of the Elastic Modulus of Ultra-High Performance Concrete using Vibration Data," *Engineering, Technology & Applied Science Research*, vol. 14, no. 4, pp. 15447–15453, Aug. 2024, https://doi.org/10.48084/etasr.7859.

[8] H. Zui, T. Shinke, and Y. Namita, "Practical Formulas for Estimation of Cable Tension by Vibration Method," *Journal of Structural Engineering*, vol. 122, no. 6, pp. 651–656, Jun. 1996, https://doi.org/10.1061/(ASCE)0733-9445(1996)122:6(651).

[9] A. B. Mehrabi and H. Tabatabai, "Unified Finite Difference Formulation for Free Vibration of Cables," *Journal of Structural Engineering*, vol. 124, no. 11, pp. 1313–1322, Nov. 1998, https://doi.org/10.1061/(ASCE)0733-9445(1998)124:11(1313).

[10] W. H. P. Yen, A. B. Mehrabi, and H. Tabatabai, "Evaluation of stay cable tension using a non-destructive vibration technique," in *Building to Last*, 1997, pp. 503–507.

[11] D.-H. Choi and W.-S. Park, "Tension force estimation of extradosed bridge cables oscillating nonlinearly under gravity effects," *International Journal of Steel Structures*, vol. 11, no. 3, pp. 383–394, Sep. 2011, https://doi.org/10.1007/s13296-011-3012-0.

[12] S. E. Haji Agha Mohammad Zarbaf, M. Norouzi, R. Allemang, V. Hunt, A. Helmicki, and C. Venkatesh, "Vibration-based cable condition assessment: A novel application of neural networks," *Engineering Structures*, vol. 177, pp. 291–305, Dec. 2018, https://doi.org/10.1016/j.engstruct.2018.09.060.

[13] T. Gai, D. Yu, S. Zeng, and J. C.-W. Lin, "An optimization neural network model for bridge cable force identification," *Engineering Structures*, vol. 286, Jul. 2023, Art. no. 116056, https://doi.org/10.1016/j.engstruct.2023.116056.

[14] J. Piao *et al.*, "Indirect Force Control of a Cable-Driven Parallel Robot: Tension Estimation using Artificial Neural Network trained by Force Sensor Measurements," *Sensors*, vol. 19, no. 11, Jan. 2019, Art. no. 2520, https://doi.org/10.3390/s19112520.

[15] S. Jeong, H. Kim, J. Lee, and S.-H. Sim, "Automated wireless monitoring system for cable tension forces using deep learning," *Structural Health Monitoring*, vol. 20, no. 4, pp. 1805–1821, Jul. 2021, https://doi.org/10.1177/1475921720935837.

[16] S.-W. Kim, B.-G. Jeon, J.-H. Cheung, S.-D. Kim, and J.-B. Park, "Stay cable tension estimation using a vision-based monitoring system under various weather conditions," *Journal of Civil Structural Health Monitoring*, vol. 7, no. 3, pp. 343–357, Jul. 2017, https://doi.org/10.1007/s13349-017-0226-7.

[17] T. Shimada, "Estimating method of cable tension from natural frequency of high mode," *Doboku Gakkai Ronbunshu*, vol. 1994, no. 501, pp. 163–171, Oct. 1994, https://doi.org/10.2208/jscej.1994.501_163.

[18] Y.-H. Huang, J.-Y. Fu, R.-H. Wang, Q. Gan, and A.-R. Liu, "Unified Practical Formulas for Vibration-Based Method of Cable Tension Estimation," *Advances in Structural Engineering*, vol. 18, no. 3, pp. 405–422, Mar. 2015, https://doi.org/10.1260/1369-4332.18.3.405.

[19] S. Cho, C.-B. Yun, and S.-H. Sim, "Evaluation of Cable Tension Forces Using Vibration Method for a Cable-stayed Bridge under Construction," *Journal of the Korean Society of Safety*, vol. 29, no. 2, pp. 38–44, 2014, https://doi.org/10.14346/JKOSOS.2014.29.2.038.